Ion target impact energy during Type I ELMs in JET ITER-like Wall

*C. Guillemaut[1,4], A. Jardin[2], J. Horacek[3], A. Autricque[2], G. Arnoux[4], J. Boom[5], S. Brezinsek[6], J.W. Coenen[6], E. De La Luna[7], S. Devaux[8], T. Eich[5], C. Giroud[4], D.Harting[4], A. Kirschner[6], B. Lipschultz[9], G.F. Matthews[4], D. Moulton[4], M. O'Mullane[10], M. Stamp[4] and JET contributors**

EUROfusion Consortium, JET, Culham Science Centre, Abingdon, OX14 3DB, UK
[1]Instituto de Plasmas e Fusão Nuclear, Instituto Superior Técnico, Universidade Lisboa, PT
[2]CEA, IRFM, F-13108 Saint-Paul-lez-Durance, France
[3]IPP.CR, Institute of Plasma Physics AS CR, Za Slovankou 3, 182 21 Praha 8, Czech Republic
[4]CCFE, Culham Science Centre, Abingdon OX14 3DB, UK
[5]Max-Planck-Institut fur Plasmaphysik, Boltzmannstr. 2, D-85748 Garching, Germany
[6]Instiut für Energie und Klimaforschung - Plasmaphysik, Forschungszentrum Jülich, 52425 Jülich, Germany
[7]Laboratorio Nacional de Fusión,CIEMAT, 28040 Madrid, Spain
[8]Institut Jean Lamour, UMR7198 CNRS - Université de Lorraine, F-54506 Vandoeuvre-les-Nancy Cedex, France.
[9]YPI, University of York, York YO10 5DQ, UK
[10]Department of Physics, University of Strathclyde, Glasgow G4 0NG, UK

Abstract

The ITER baseline scenario, with 500 MW of DT fusion power and Q = 10, will rely on a Type I ELMy H-mode, with ΔW = 0.7 MJ mitigated ELMs. Tungsten (W) is the material now decided for the divertor plasma-facing components from the start of plasma operations. W atoms sputtered from divertor targets during ELMs are expected to be the dominant source under the partially detached divertor conditions required for safe ITER operation. W impurity concentration in the plasma core can dramatically degrade its performance and lead to potentially damaging disruptions. Understanding the physics of plasma-wall interaction during ELMs is important and a primary input for this is the energy of incoming ions during an ELM event. In this paper, coupled Infrared thermography and Langmuir Probe (LP) measurements in JET-ITER-Like-Wall unseeded H-mode experiments with ITER relevant ELM energy drop have been used to estimate the impact energy of deuterium ions (D^+) on the divertor target. This analysis gives an ion energy of several keV during ELMs, which makes D^+ responsible for most of the W sputtering in unseeded H-mode discharges. These LP measurements were possible because of the low electron temperature (T_e) during ELMs which allowed saturation of the ion current. Although at first sight surprising, the observation of low T_e at the divertor target during ELMs is consistent with the "Free-Streaming" kinetic model which predicts a near-complete transfer of parallel energy from electrons to ions in order to maintain quasi-neutrality of the ELM filaments while they are transported to the divertor targets.

Corresponding Email: christophe.guillemaut@ccfe.ac.uk or cguillemaut@ipfn.ist.utl.pt

* See the Appendix of F. Romanelli et al., Proceedings of the 25th IAEA Fusion Energy Conference 2014, Saint Petersburg, Russia

1. Introduction

The ITER baseline scenario, with 500 MW of DT fusion power and Q = 10, will rely on a Type I ELMy H-mode, with ΔW = 0.7 MJ mitigated ELMs, see [1]. Partial divertor detachment with nitrogen (N), neon (Ne) or argon (Ar) impurity seeding will also be required to maintain the inter-ELM power load at managable level. Tungsten (W) is the material now decided for the divertor plasma-facing components from the start of plasma operations. Under the partially detached divertor conditions envisaged for ITER, W atoms sputtered from divertor targets during ELMs are expected to be the dominant impurity source. In ITER, W impurity concentration in the plasma core above 5 x 10^{-5} can degrade fusion performance and may lead to potentially damaging disruptions, see [2]. Understanding the physics of plasma-wall interaction during ELMs is important and a primary input for this is the energy of incoming ions during an ELM event.

The JET-ITER-Like-Wall (JET-ILW) [3] comprises a W divertor and beryllium (Be) main chamber wall thus matching the material configuration planned for ITER. Due to the high energy threshold for physical sputtering of W by deuterium ions (D^+), the dominant Be ion species, Be^{2+}, contributes to W sputtering in the divertor between ELMs (inter-ELM), see [4]. During ELM events, sputtering by D^+ could significantly contribute to W sputtering if the impact energy is sufficiently high and the concentration of Be is as low as observed in the JET-ILW. As an example, according to TRIM calculations for perpendicular impact [5] shown on Fig. 1, if Be^{2+} and D^+ both have a target impact energy (E_i) of ~ 1 keV, they rise their respective W sputtering yield up to $Y_{Be/W}$ ~ 0.1 and $Y_{D/W}$ ~ 0.01. According to [4], in most JET-ILW experiments, the Be concentration in the impinging target ion flux is ~ 0.5 % which means that D^+ could potentially produce ~ 20 times more W sputtering than Be^{2+} during a Type I ELM. Therefore, determining E_i experimentally during ELMs is important for verifying whether W sputtered by D^+ is dominant or not. If it is, then the task of modelling the W source term during ELMs becomes simpler given that it is difficult to precisely measure the Be content and charge state mix in the scrape-off layer during an ELM or to predict it reliably.

A series of high power unseeded H-Mode discharges performed in JET-ILW (see Table 1) during the W melting experiments [6] has been studied for this purpose. They have been chosen for the range of pedestal electron temperatures (T_e^{ped}) they explore and for the ITER relevance of the energy of their Type I ELMs (up to ~ 0.3 MJ). The divertor configuration used in these experiments features a vertical inner target with a horizontal outer target (OT), see Fig. 2. The present work has been focused on the use of high time resolution Infrared thermography (IR), Langmuir Probes (LP) and Electron Cyclotron Emission (ECE) measurements to study the conditions on the horizontal OT during ELMs compared to the pedestal conditions.

Before discussing the experimental results, it is essential to confirm that ion saturation current densities (J_{sat}) measured by LP remain valid during ELMs by comparing to D_α spectroscopy measurements (Section 2) and by analyzing current-voltage (I-V) characteristic reconstruction from LP during ELMs (Section 3). The positive outcome of this analysis means that it is possible to estimate E_i by coupling IR and LP measurements and compare it to pedestal conditions measured by ECE (Section 4). To conclude, we discuss the consequences of these estimates on W sputtering due to D^+ and Be^{2+} (Section 5) and also the extent to which our results are consistent with the theory of ELM events as represented in kinetic models.

2. Ion flux measurements with LP and D_α spectroscopy during ELMs

It could be argued that the current measured by a single LP cannot be used during ELMs to obtain a proper J_{sat} value, since the electrons may simply have too much parallel energy to be repelled by the biased surface of the probes [7]. For example, the LP at JET cannot be biased to more than -170 V, which would be insufficient to repel electrons with a parallel energy of the order of 0.5 - 1 keV which are typical of the T_e^{ped} in JET-ILW. In this hypothetical case, the current measured by the probes would not saturate and the maximum ion flux obtained at -170 V would still be significantly lower than the real flux.

LP are routinely used in high power H-Mode JET-ILW experiments like those listed in Table 1. In these cases, the LP voltage was swept between +30 V and -140 V every 2.4 ms with an acquisition rate of 100 kHz for the current and voltage measurements. Thus, if the electrons had a sufficiently low energy to be repelled by a biased LP in the divertor, the saturated ion branch of the I-V characteristic - which last for a period of ~ 2 ms in each sweep - would provide a J_{sat} measurement with 10 μs time resolution. This should allow precise description of Type I ELMs since they typically last for a period of ~ 1 - 2 ms.

As a first verification of the accuracy of the LP ion current measurements during ELMs, a comparison has been made between the measurements from D_α spectroscopy and the set of 12 LP on the OT (Tile 5 in Fig. 2). It has been assumed that the intensity of D_α line emission from local deuterium recycling is proportional to the ion flux falling on the area of the OT seen by the filterscope equiped with narrowband D_α filters. The filterscope used to measure the D_α is absolutely calibrated and the recycling coefficient is assumed to be R = 1. In the series of experiments considered here (see Table 1), it has been found that during inter-ELM, the ratio between the integrated LP ion flux on Tile 5 (Fig. 2) and the total number of Balmer photons per second in the same field of view is ~ 20. This is consistent with previous studies on JET and expected values from ADAS [8,9] for the number of ionization per photon which is relatively independent of electron temperature (T_e) in the range ~ 30 – 1000 eV as shown in Fig. 3.

Because of their high energy and low frequency (See Table 1), the Type I ELMs obtained in these experiments are reproducible in terms of amplitude and duration and thus an ELM detection algorithm coupled with a coherent averaging method [10] has been applied to the integrated signals from LP and D_α spectroscopy to obtain a typical ELM ion flux signature for a given discharge. Intensity spikes of Be II line radiation associated with enhanced target particle and heat fluxes due to ELMs have been used as a marker signal here to define the zero of a new time base for each ELM seen by D_α spectroscopy and LP. The signals have been accumulated and averaged to yield a single coherently averaged ELM. The example given in Fig. 4 for the particular discharge #84782 is representative of the other cases listed in Table 1. It follows that the discrepancy between both measurements of ion flux is not higher than ~ 50 % during the averaged ELM phase which suggests that LP measurements seem to be accurate in these conditions.

Whilst reasonable, this level of discrepancy can be explained by the electron density (n_e) dependence of the number of ionizations per photon as shown in Fig. 3, according to ADAS [9]. As an example, in the inter-ELM attached conditions of discharge #84782, the target n_e measured at the strike point by Probe 13 (see Fig. 2) is of the order of ~ 10^{19} m^{-3}. If the target n_e increases by a factor 10 during an ELM because of strong desorption and ionization processes, Fig. 3 shows that the number of ionization per photon should evolve from ~ 20 to ~ 30 - 50 when T_e is between 30 and 1000 eV. On Fig. 4c, a better match between LP and D_α spectroscopy signals during ELMs would require a number of ionization per photon of the order of ~ 30 which is in the range of values that could be expected in these conditions.

One interesting feature of the ELMs in this series of discharges is that they are always followed by a short and intense particle pulse which is not associated with a significant power deposition, see Fig. 5. As shown by Be II and W I spectroscopy, this low energetic peak which occurs ~ 8 ms after the ELM event is not responsible for any significant sputtering on the targets. This phenomenon which may be related to thermal desorption of gas stored in the surface [4,11] is very common in JET-ILW and has also been observed on ASDEX-Upgrade.

Similar particle fluxes measured by LP and D_α spectroscopy during ELMs is an indication that the parallel energy of the electrons at the targets may be sufficiently low to allow their repulsion by the biased LP surfaces and therefore the saturation of the measured current when the applied voltage is high enough. If there was no current saturation during ELMs, the ion flux measured by the LP should be much lower than the D_α spectroscopy measurement on Fig. 4c. It is therefore a positive result to see that the opposite situation occurs in reality. Better evidence would be the direct observation of LP current saturation during ELMs which is the subject of the next Section.

3. Direct observation of LP current saturation during ELMs

As an example, peak ELM current values (I in A) with their associated voltages (V in V) have been accumulated over the entire discharge #84782 for the LP closest to the strike point (see Probe 13 on Fig. 2) to reconstruct the typical I-V characteristic associated with these conditions. The standard exponential 3-parameter fit, equation (1), has been applied to the coherently averaged raw data where T_e is in eV, the floating potential V_f is in V and the ion saturation current I_{sat} is in A:

$$I = I_{sat}(1 - \mathrm{e}^{\frac{V - V_f}{T_e}}). \qquad (1)$$

As shown on Fig. 6, it appears that in these conditions, the I-V characteristic reconstruction from Probe 13 does saturate. The associated target T_e is of the order of ~ 20 – 30 eV, which is sufficiently low to allow the repulsion of the electrons and an accurate measurement of the target ion flux during ELMs, as already suggested by the comparison with D_α measurements. It is worth mentioning that target T_e of the same order of magnitude have already been observed on TCV during ELMs [10] using the same method.

As shown on Fig. 7, before the ELM, T_e^{ped} measured by ECE is of the order of ~ 1 keV which makes the observation at first sight rather surprising given that during an ELM one can think that the divertor target becomes connected along a magnetic flux tube to a plasma with the same T_e as the pedestal. However, low target T_e during ELMs – of the order of the inter-ELM value – are actually consistent with the “Free-Streaming” model for the description of parallel ELM transport, see [12-14]. The quasi-neutrality of ELM filament parallel transport forces the electrons to transfer most of their parallel energy to the ions on their way to the targets to avoid the appearance of strong electric fields between two decoupled populations of ions and electrons. Therefore, the quasi-neutral ELM filaments are expected to strike the targets with high parallel energy ions and low parallel energy electrons.

Thus, the coupling of accurate high time resolution particle flux measurements from the LP and heat flux measurements from IR cameras should in principle give access to reasonable estimates of E_i during Type I ELMs.

4. E_i estimates during ELMs and relation with pedestal conditions

Fast LP and IR camera measurements have a time resolution of respectively 10 μs for J_{sat} and 200 μs for perpendicular power density ($q_\perp$) which should be sufficient to resolve the Type I ELMs (~ 1 - 2 ms duration) for the series of discharges listed in Table 1. Since both measurements appear to be reliable during ELMs (see [15] for the use of IR in these conditions) they can be coupled to estimate the sum of the electron energy (E_e)

and E_i. In the series of experiments of Table 1, Z_{eff} ~ 1.1 – 1.3, thus the ion density is close to n_e and $E_i + E_e$ in eV can be obtained as follows:

$$E_i + E_e = \frac{q_\perp}{J_{sat}\sin\theta_\perp}, \tag{2}$$

with $\theta_\perp$ the field line angle on the OT (~ 2 - 3º here). Since in JET-ILW, the fast IR camera looks mainly at the OT which has the best LP coverage, the present study has been focused on this particular area of the divertor.

As already described, the respective J_{sat} and $q_\perp$ measurements from LP and IR at the strike point position (Probe 13 in Fig. 2) have been coherently averaged over the discharge #84782 to obtain the typical ELMy $E_i + E_e$ signature shown in Fig. 8. More than ~ 200 ELMs have been cumulated and this averaging starts 2 ms before each ELM event and ends 5 ms after. In this example, it can be seen that the peak of $E_i + E_e$ during the ELM and the T_e^{ped} before the ELM crash ($T_{e,\max}^{ped}$) are such that:

$$\max(E_i + E_e) \approx \alpha T_{e.\max}^{ped}. \tag{3}$$

Both values have been compared for the other discharges of Table 1 using the same ELM detection algorithm and coherent averaging method and the result is shown on Fig. 9. According to the linear fit (red dotted line), the simple linear dependence shown in (3) describes quite well the experimental behavior if $\alpha \approx 5.25$. Even if the error bars on Fig. 9 are significant, this is in excellent agreement with the "Free-Streaming" model [12-14]. Indeed, the latter predicts a factor α = 5.23 between $max(E_i + E_e)$ and $T_{e,\max}^{ped}$ if in [14] equation (36) is inserted in equation (34) and if the ion pedestal temperature (T_i^{ped}) is such that $T_i^{ped} \approx T_e^{ped}$, as confirmed by edge charge-exchange spectroscopy and ECE measurements. Since the electron parallel energy is almost entirely transferred to the ions on their way to the target, the model assumes that the perpendicular electron energy ($E_{e,\perp}$) is the only component left in E_e such that:

$$E_e = E_{e,\perp} = T_e^{ped}. \tag{4}$$

Thus, the maximum value of E_i during ELMs ($E_{i,max}$) is:

$$E_{i,\max} = (\alpha - 1)T_{e,\max}^{ped} = 4.23T_{e,\max}^{ped}. \tag{5}$$

This means that $T_{e,\max}^{ped}$ seems to be the only information required to have access to $E_{i,max}$ during ELMs.

5. Dominant contribution from D^+ to W sputtering

Now that E_i can be experimentally determined for the main plasma species, the relative importance of the different W sputtering processes occurring in the unseeded H-mode discharges studied here (see Table 1) can be calculated. Some simplifications will be made to facilitate the analysis and focus the discussion on the orders of magnitude of the W sputtering due to D^+ and Be^{2+} in ELM and inter-ELM conditions.

It can be deduced from (5) and $T_{e,\max}^{ped}$ measurements on Fig. 9 that $E_{i,max}$ for D^+ has an average of ~ 3 keV and ranges from ~ 2 keV to ~ 4 keV during Type I ELMs in JET-ILW unseeded H-modes. In inter-ELM it is considered, as in [4], that the ion impact energy ($E_{i,inter\text{-}ELM}$), T_e, and the target ion temperature (T_i) are such that:

$$E_{i,\mathrm{inter}-ELM} = 3T_e + 2T_i \,. \tag{6}$$

Since here $T_i \approx T_e \approx 20 - 30$ eV at the OT in inter-ELM (see Section 3), $E_{i,inter\text{-}ELM}$ should not be higher than ~ 150 eV.

In ELM and inter-ELM conditions it is pessimistically assumed that the ion impact energy is the same for D^+ and Be^{2+}. As shown on Fig. 10 obtained from TRIM [5] calculations, the ion impact angle with the divertor targets (θ_i) is expected to have a strong influence on the W sputtering yield.

In inter-ELM, θ_i depends on the ion velocity distribution and the sheath effects at the target. The calculation of the actual distribution of θ_i is not required for the present discussion which is focused on orders of magnitudes only but it should be the object of further studies. Since $E_{i,inter\text{-}ELM}$ ~ 150 eV, $Y_{D/W}$ is negligible (see Fig. 1) and it confirms that W sputtered by Be^{2+} and other Be species – all contributing in the same way – is the dominant sputtering process during inter-ELM, as already discussed in [4].

In [14] it is shown that in a simple 1D model of a plasma bunch expending into vacuum, the electrons transfer most of their parallel energy to the ions during ELMs to maintain quasi-neutrality. Thus, they do not have enough energy left to establish a significant sheath at the target. Here, we tentatively extend this result to a real ELM and assume that the angle of incidence of the ion guiding center with the target is $\theta_\perp$ during ELMs. In the absence of a sheath, the distribution of θ_i depends on the velocity distribution in the perpendicular direction. Therefore, θ_i for each ELMy ion could vary between a few degrees and normal incidence. As for the inter-ELM case, the calculation of the distribution of θ_i for ELMy ions has not been considered since it is not required for the present discussion.

With θ_i between a few degrees and normal incidence and $E_{i,max}$ ~ 3 keV in average, Fig. 10 shows that $Y_{D/W}$ and $Y_{Be/W}$ vary strongly. At normal incidence, $Y_{Be/W}$ is one order of magnitude stronger than $Y_{D/W}$ and at shallow θ_i, both sputtering yields are approximately equal.

According to Fig. 4, the average OT perpendicular ion flux increases by a factor ~ 4 between the inter-ELM phase and the ELM phase and the Be concentration in the impinging target ion flux is ~ 0.5% [4]. Thus, if ion fluxes are normalized to the peak perpendicular OT ELMy D^+ flux (~ 8 x 10^{23} s^{-1} on Fig. 4c) and multiplied by the sputtering yield of Fig. 10, the typical angular variations of normalized OT W sputtering fluxes due to D^+ and Be^{2+} in ELM and inter-ELM conditions are obtained on Fig. 11. Estimates are only provided for the W sputtering source. The small fraction reaching the plasma core because of prompt W redeposition has not been estimated here.

If it is assumed that the inter-ELM phase with constant E_i at $E_{i,inter\text{-}ELM}$ = 150 eV is ~ 10 times longer than the ELM phase (Fig. 4) with constant E_i at $E_{i,max}$ = 3 keV, the integrated amount of W sputtered by D^+ and Be^{2+} over a Type I ELM cycle in JET-ILW can be evaluated as follows:

$$\int_{Cycle} \Gamma_W \, dt \approx \left(\Gamma_{D^+,ELM} Y_{D/W}(3k\,\mathrm{eV}) + \Gamma_{Be^{2+},ELM} Y_{Be/W}(3k\,\mathrm{eV}) + 10\Gamma_{Be^{2+},\mathrm{inter}-ELM} Y_{Be/W}(150\,\mathrm{eV}) \right) \Delta t_{ELM} , \quad (7)$$

where Δt_{ELM} is the average ELM duration in s and Γ_W , $\Gamma_{D^+,ELM}$, $\Gamma_{Be^{2+},ELM}$ and $\Gamma_{Be^{2+},\mathrm{inter}-ELM}$ are the sputtered W flux, the ELMy D^+ flux, the ELMy Be^{2+} flux and the inter-ELM Be^{2+} flux respectively in s^{-1}. By using the different contributions to W sputtering from Fig. 11 (multiplied by the peak OT ELMy D^+ flux) to solve (7), it follows that the integrated amount of W sputtering due to Be^{2+} (last two terms in (7)) is ~ 10 to ~ 100 times lower than the integrated amount of W sputtered by D^+ (first term in (7)) over an ELM cycle. Therefore, the W sputtering in unseeded H-mode, discharges in JET-ILW is dominantly due to D^+ during ELMs because of the low Be concentration in the impinging target ion flux.

Thus, the choice of Be as plasma facing material for the main chamber seems to have very limited impact on W sputtering in the divertor in JET-ILW which is encouraging for ITER. However, W sources during ELMs are expected to increase with the mass of the main plasma species (e.g. DT and He plasmas), see Fig.1. The use of N, Ne or Ar impurity seeding for partially detached divertor operation to reduce the target heat flux is also expected to participate to W sputtering [16] but this case has not been studied here.

6. Conclusions

Mitigated Type I ELMs, with ΔW = 0.7 MJ of energy, expected in ITER for the baseline scenario with 500 MW of fusion power and Q = 10, are expected to be the dominant source of W in ITER. Very small amounts of W will be tolerated in the plasma core to ensure good performance [2]. Therefore, it is critical to predict accurately the W source due to ELM sputtering and this means that the energy of the incident ions needs to be known.

Coupled IR and LP measurements in JET-ILW Type I ELMy H-mode experiments with ITER relevant ELM energy drop have been used here to confirm that D^+ have sufficient impact energy during ELMs to be the main responsible species for W sputtering when no extrinsic impurity seeding is involved. In the series of discharges studied here, it appears that $E_{i,max}$ during ELMs is in the range 2 – 4 keV for D^+ and has a simple linear dependence on $T_{e,\max}^{ped}$.

Comparison of LP with D_α ion flux measurements and analysis of reconstructed I-V characteristics during ELMs have been presented to prove that the ion current does saturate in these conditions. Thus, J_{sat} measurements during ELMs are accurate and it is therefore reasonable to couple it to IR measurements for E_i estimates.

The saturation of the ion current measured by the LP during ELMs is possible thanks to the surprisingly low T_e of the order of ~ 20 - 30 eV (similar to inter-ELM conditions) found by the fit of the reconstructed I-V characteristic. These results are consistent with the predictions of the “Free-Streaming” model for the description of parallel ELM transport [12-14]. According to the model, electrons have to transfer most of their parallel energy to the ions on their way to the target to maintain the quasi-neutrality of the ELM filaments. The remaining low energy ELMy electrons are therefore easy to repel by the biased LP at the targets, making the ion flux measurement possible during ELMs.

This study indicates that the choice of Be as plasma facing material for the main chamber have very limited impact on W sputtering in the divertor in JET-ILW because of its low concentration in the plasma. Since the main species seems to be responsible for most of the W sputtering in H-mode unseeded JET-ILW experiments, W sources during ELMs are likely to increase with the mass of the main plasma species (e.g. DT and He plasmas) according to the standard formula for the physical sputtering yield.

Acknowledgments

This work has been carried out within the framework of the EUROfusion Consortium and has received funding from the Euratom research and training programme 2014-2018 under grant agreement No 633053 and the MSMT INGO grant LG14002. IST activities also received financial support from “Fundação para a Ciência e Tecnologia” through project UID/FIS/50010/2013. The views and opinions expressed herein do not necessarily reflect those of the European Commission.

References

[1] A. Loarte et al., Nucl. Fusion **54** (2014) 033007

[2] A. Kallenbach et al., Plasma Phys. Control. Fusion **47** (2005) B207–B222
[3] G.F. Matthews et al., 2011 Phys. Scr. 2011 014001
[4] S. Brezinsek et al., PSI 2014
[5] W. Eckstein et al., Report IPP 9/132 (2002)
[6] J.W. Coenen et al., PSI 2014
[7] D. Tskhakaya et al., J. Nucl. Mater. **415** (2011) S860–S864
[8] M.F. Stamp et al., Physica Scripta vol. **T91** (2001) 13
[9] H.P. Summers. *Atomic data and analysis structure user manual*. University of Strathclyde, 2nd edition, 2004
[10] R.A. Pitts et al., Nucl. Fusion **43** (2003) 1145–1166
[11] M. Wischmeier et al., J. Nucl. Mater. **363–365** (2007) 448–452
[12] W. Fundamenski et al., Plasma Phys. Control. Fusion **48** (2006) 109–156
[13] T. Eich et al., J. Nucl. Mater. **390–391** (2009) 760–763
[14] D. Moulton et al., Plasma Phys. Control. Fusion **55** (2013) 085003
[15] T. Eich et al., J. Nucl. Mater. **415** (2011) S856–S859
[16] G.J. van Rooij et al., J. Nucl. Mater. **438**, Supplement, (2013) S42–S47

Table Captions:

Table 1 List of unseeded H-mode JET-ILW discharges studied here

Figure captions:

Fig. 1 Curves of W sputtering yields at normal incidence due to Be in red, helium (He) in green, tritium (T) in magenta and deuterium (D) in blue.

Fig. 2 Left: positions of LP and IR camera line of sight in JET-ILW divertor with the different Tile numbers. Right: magnetic equilibrium for #84782 at 13 s and position of D_α spectroscopy and ECE lines of sight in JET-ILW main chamber.

Fig. 3 Number of ionizations per D_α photon obtained from ADAS [9].

Fig. 4 (a) Total OT ion flux form LP, (b) Total OT ion flux deduced from D_α spectroscopy, (c) Coherently averaged total OT ion flux from LP (blue data points) and calibrated D_α spectroscopy (red data points) with respective standard deviation over the cumulated ELM cycles of #84782, (d) discrepancy between both curves.

Fig. 5 (a) Coherently averaged total OT power measured by the IR camera over the cumulated ELM cycles of #84782, (b) same as previously with the intensity of D_α, Be II and W I line radiation (note that for convenience, the scale for Be II and W I is 100 time lower than the scale for D_α). All error bars represent the standard deviation.

Fig. 6 I-V characteristic reconstruction obtained by cumulating I and V measurements taken by the LP in the peak ELMy ion flux of each ELM event over the discharge #84782.

Fig. 7 Coherently averaged T_e^{ped} with standard deviation measured by ECE over the cumulated ELM cycles of #84782.

Fig. 8 Coherently averaged (a) local $q_\perp$ measured from IR for Probe 13 position, (b) J_{sat} measurement by Probe 13, (c) T_e^{ped} from ECE and E_i+E_e deduced from LP and IR measurements over the cumulated ELM cycles of #84782. All error bars represent the standard deviation.

Fig. 9 $max(E_i+E_e)$ in function of $T_{e,\max}^{ped}$ from coherent averaging of LP, IR and ECE measurements obtained in the discharges listed in Table 1. The equation for the linear fit is y = 5.25 x (red dotted line) while the theory predict y = 5.23 x (black plain line).

Fig. 10 θ_i dependence of W sputtering yield due to D^+ (blue curve) and Be^{2+} (red curves) for E_i = 150 eV (dashed) and E_i = 3000 eV (plain).

Fig. 11 θ_i dependence of W sputtering flux due to D^+ (blue curve) and Be^{2+} (red curves) for E_i = 150 eV (dashed) and E_i = 3000 eV (plain) and normalized to the maximum ELMy OT D^+ flux.

Pulse number	P_{NBI} (MW)	B_t (T)	I_p (MA)	T_e^{ped} (eV)	ΔW (kJ)	f_{ELM} (Hz)
#84589	12	2	2	697	122	45
#84593	12	2	2	498	119	49
#84613	13	2	2	599	125	43
#84614	13	2	2	548	120	46
#84722	20	3	3	801	141	67
#84724	19	3	3	749	175	31
#84778	21	3	3	982	211	37
#84779	21	3	3	854	222	26
#84782	21	3	3	1053	191	39

Table 1

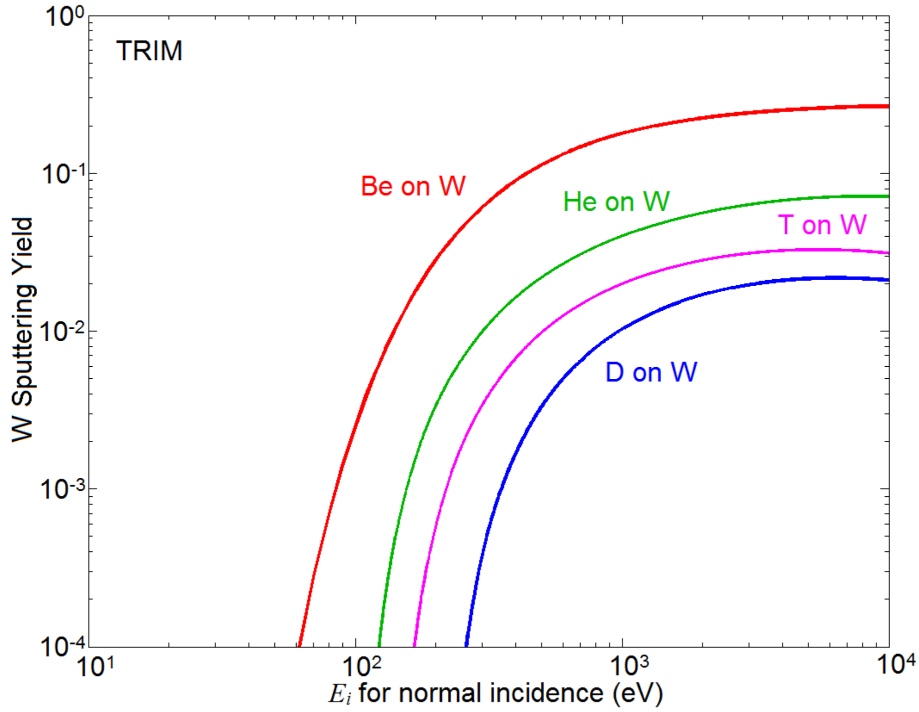

TRIM
Be on W
He on W
T on W
D on W
W Sputtering Yield
E_i for normal incidence (eV)
10^0
10^-1
10^-2
10^-3
10^-4
10^1
10^2
10^3
10^4

Figure 1

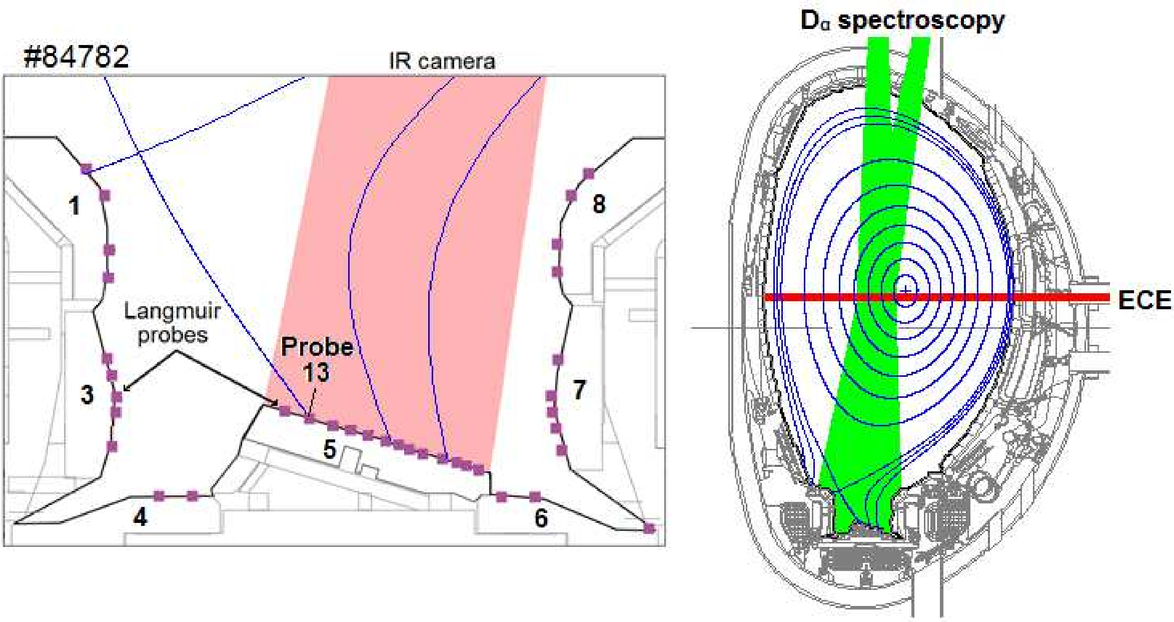

#84782
IR camera
1
8
Langmuir
probes
Probe
13
3
7
5
4
6
Dα spectroscopy
ECE

Figure 2

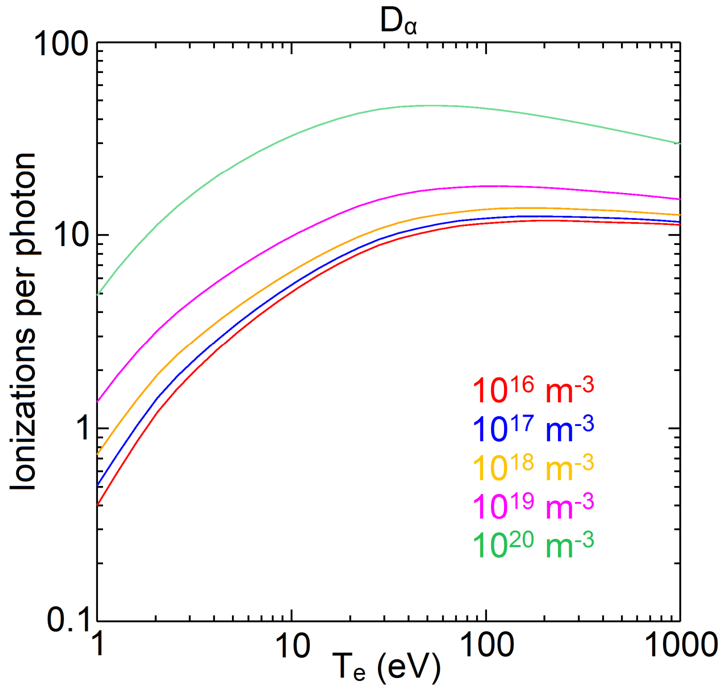
Dα
100
10
1
0.1
1
10
100
1000
Ionizations per photon
Te (eV)
10^16 m^-3
10^17 m^-3
10^18 m^-3
10^19 m^-3
10^20 m^-3

Figure 3

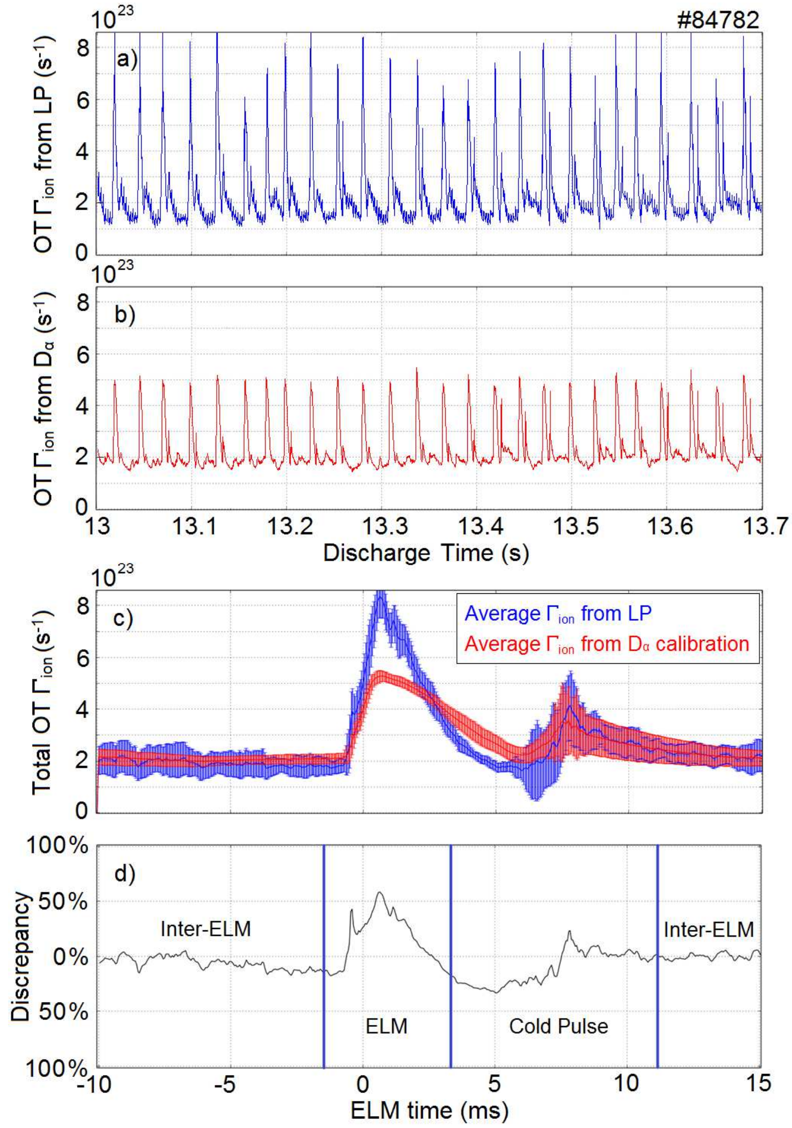
#84782
a)
b)
c)
d)
OT Γion from LP (s-1)
OT Γion from Dα (s-1)
Discharge Time (s)
Total OT Γion (s-1)
Average Γion from LP
Average Γion from Dα calibration
Discrepancy
Inter-ELM
ELM
Cold Pulse
Inter-ELM
ELM time (ms)

Figure 4

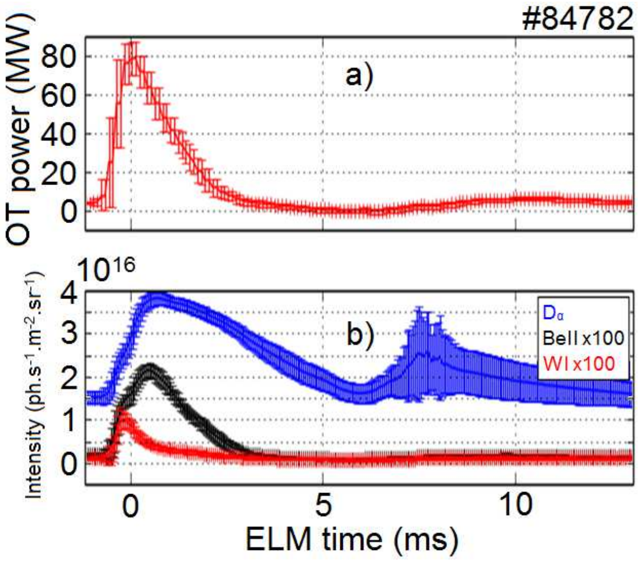

#84782
OT power (MW)
a)
80
60
40
20
0
10^16
Intensity (ph.s^-1.m^-2.sr^-1)
b)
4
3
2
1
0
Dα
BeII x100
WI x100
0
5
10
ELM time (ms)

Figure 5

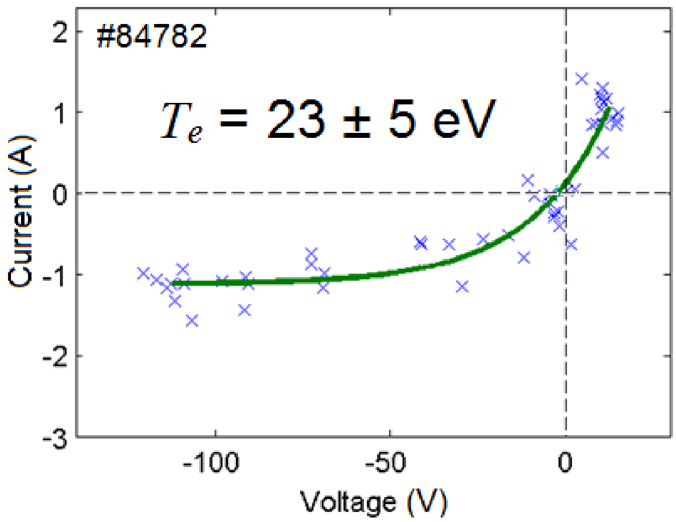

Figure 6

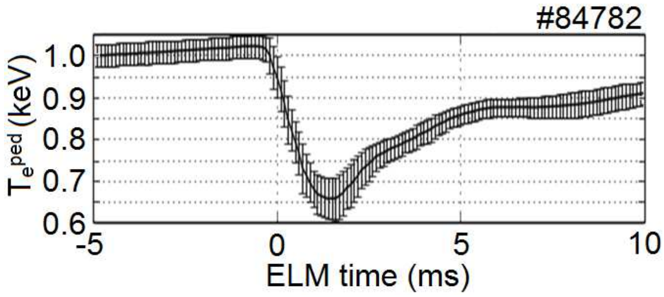

Figure 7

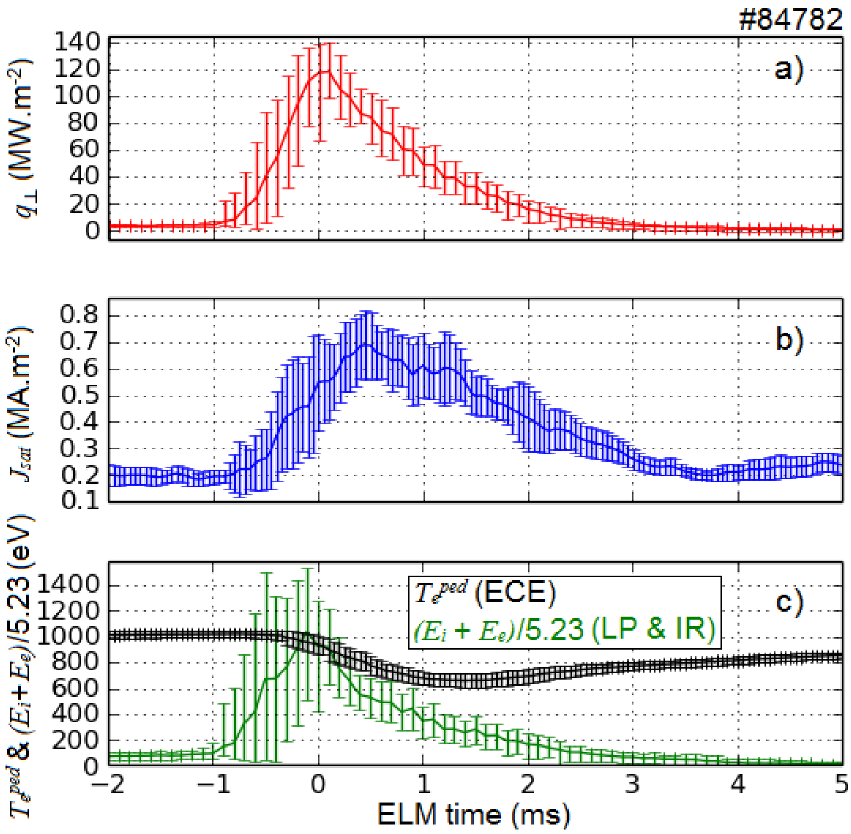

#84782
a)
b)
c)
$q_\perp$ (MW.m^{-2})
J_{sat} (MA.m^{-2})
T_e^{ped} & (E_i+E_e)/5.23 (eV)
T_e^{ped} (ECE)
$(E_i + E_e)$/5.23 (LP & IR)
ELM time (ms)

Figure 8

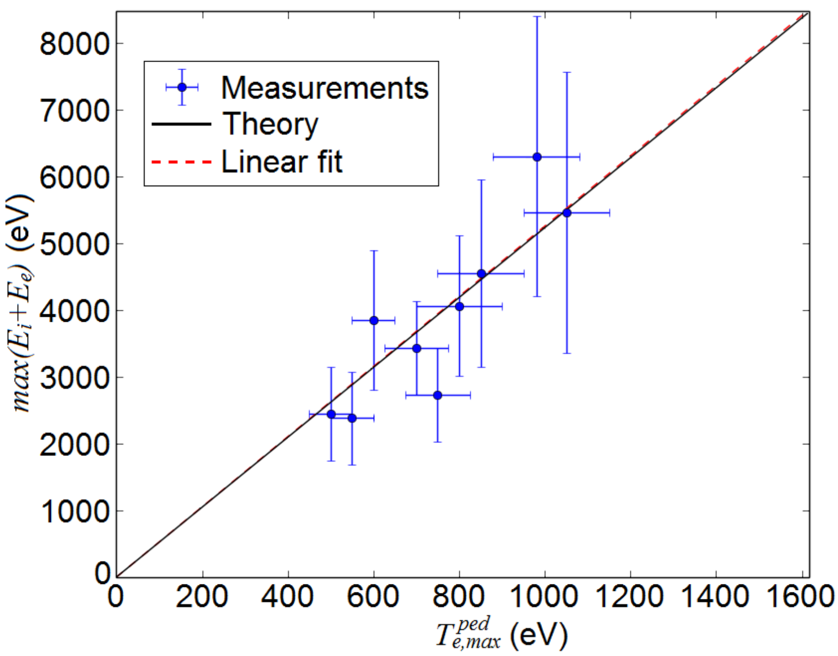

Measurements
Theory
Linear fit
8000
7000
6000
5000
4000
3000
2000
1000
0
0
200
400
600
800
1000
1200
1400
1600
$max(E_i+E_e)$ (eV)
$T_{e,max}^{ped}$ (eV)

Figure 9

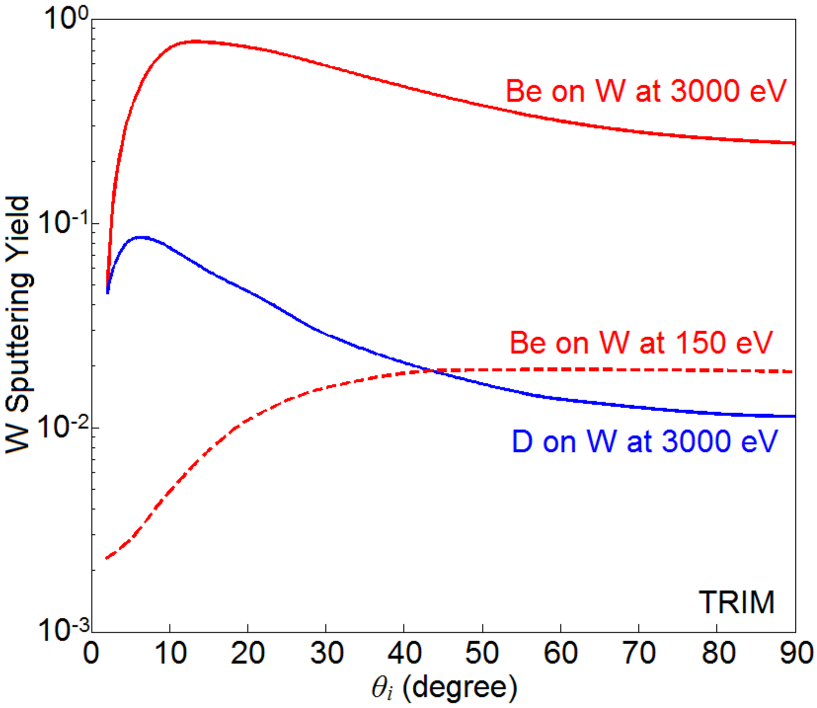

Be on W at 3000 eV
Be on W at 150 eV
D on W at 3000 eV
TRIM
W Sputtering Yield
θ_i (degree)

Figure 10

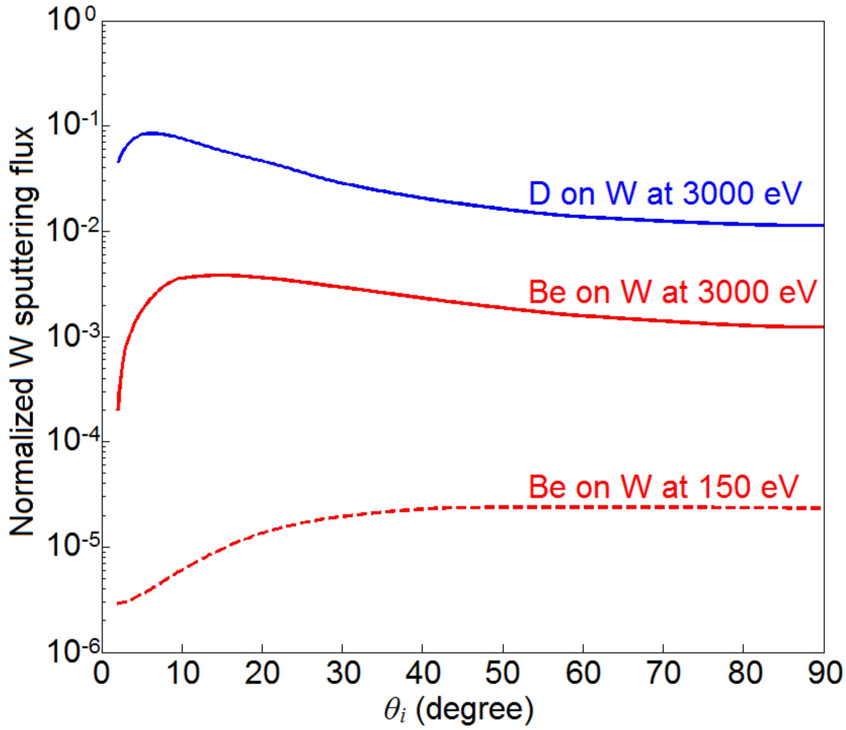

Normalized W sputtering flux
D on W at 3000 eV
Be on W at 3000 eV
Be on W at 150 eV
θi (degree)

Figure 11